RNA-Sequencing Analysis Revealed a Distinct Motor Cortex Transcriptome in Spontaneously Recovered Mice After Stroke

Masaki Ito, MD, PhD*; Markus Aswendt, PhD*; Alex G. Lee, PhD; Shunsuke Ishizaka, MD, PhD; Zhijuan Cao, PhD; Eric H. Wang, BS; Sabrina L. Levy, BS; Daniel L. Smerin, BS; Jennifer A. McNab, PhD; Michael Zeineh, MD, PhD; Christoph Leuze, PhD; Maged Goubran, PhD; Michelle Y. Cheng, PhD†; Gary K. Steinberg, MD, PhD†

Background and Purpose—Many restorative therapies have been used to study brain repair after stroke. These therapeutic-induced changes have revealed important insights on brain repair and recovery mechanisms; however, the intrinsic changes that occur in spontaneously recovery after stroke is less clear. The goal of this study is to elucidate the intrinsic changes in spontaneous recovery after stroke, by directly investigating the transcriptome of primary motor cortex in mice that naturally recovered after stroke.

Methods—Male C57BL/6J mice were subjected to transient middle cerebral artery occlusion. Functional recovery was evaluated using the horizontal rotating beam test. A novel in-depth lesion mapping analysis was used to evaluate infarct size and locations. Ipsilesional and contralesional primary motor cortices (iM1 and cM1) were processed for RNA-sequencing transcriptome analysis.

Results—Cluster analysis of the stroke mice behavior performance revealed 2 distinct recovery groups: a spontaneously recovered and a nonrecovered group. Both groups showed similar lesion profile, despite their differential recovery outcome. RNA-sequencing transcriptome analysis revealed distinct biological pathways in the spontaneously recovered stroke mice, in both iM1 and cM1. Correlation analysis revealed that 38 genes in the iM1 were significantly correlated with improved recovery, whereas 74 genes were correlated in the cM1. In particular, ingenuity pathway analysis highlighted the involvement of cAMP signaling in the cM1, with selective reduction of Adora2a (adenosine receptor A2A), Drd2 (dopamine receptor D2), and Pde10a (phosphodiesterase 10A) expression in recovered mice. Interestingly, the expressions of these genes in cM1 were negatively correlated with behavioral recovery.

Conclusions—Our RNA-sequencing data revealed a panel of recovery-related genes in the motor cortex of spontaneously recovered stroke mice and highlighted the involvement of contralesional cortex in spontaneous recovery, particularly Adora2a, Drd2, and Pde10a-mediated cAMP signaling pathway. Developing drugs targeting these candidates after stroke may provide beneficial recovery outcome.

Visual Overview—An online visual overview is available for this article. **(*Stroke*. 2018;49:2191-2199. DOI: 10.1161/STROKEAHA.118.021508.)**

Key Words: motor cortex ■ recovery of function ■ stroke ■ transcriptome

Stroke is one of the leading causes of disability worldwide.[1] Treatment for enhancing stroke recovery is limited and most survivors remain disabled with chronic impairments, especially in patients with severe initial deficit.[2] Spontaneous recovery after stroke has been reported in both human and animal studies.[3–8] The degree of recovery can be variable and depends on several factors, such as infarct size/locations, severity of initial stroke deficits, age, and genetics.[7] Extensive studies have characterized brain repair mechanisms after stroke, mostly focused on changes in the peri-infarct regions. These include neurogenesis, angiogenesis, gliogenesis, dendritic spine turnover, axonal sprouting, growth factor release, and neuroinflammation.[7,9–14] Increasing evidence using restorative treatments have also revealed how various pharmacological, cell transplantation, rehabilitation, and brain stimulation treatments can enhance these repair mechanisms and promote

Received March 16, 2018; final revision received May 23, 2018; accepted June 28, 2018.

From the Department of Neurosurgery (M.I., M.A., S.I., Z.C., E.H.W., S.L.L., D.L.S., M.Y.C., G.K.S.), Department of Pediatrics (A.G.L.), and Department of Radiology (J.A.M., M.Z., C.L., M.G.), Stanford University School of Medicine, CA.

*Drs Ito and Aswendt contributed equally.

†Drs Steinberg and Cheng are co-senior authors and shared corresponding authorship.

The online-only Data Supplement is available with this article at https://www.ahajournals.org/doi/suppl/10.1161/STROKEAHA.118.021508.

Correspondence to Gary K. Steinberg, MD, PhD, Department of Neurosurgery, Stanford University Medical Center, 300 Pasteur Dr, R301A, MC 5325, Stanford, CA 94305, Email gsteinberg@stanford.edu or Michelle Y. Cheng, PhD, Department of Neurosurgery, Stanford University, 1201 Welch Rd, MSLS P352, Stanford, CA 94305, Email mycheng@stanford.edu

recovery after stroke,[13,15–17] providing important insights on poststroke recovery mechanisms. In the recent years, there has been increased focus on changes beyond the peri-infarct regions, as stroke causes network-wide changes in the brain.[18–20] Human and animal studies have reported functional and structural changes in the contralesional cortex, suggesting that stroke-connected brain regions such as contralesional cortex may be involved in brain repair and recovery after stroke.

In this study, our goal is to elucidate the intrinsic mechanisms of spontaneous recovery after stroke without any external intervention. To achieve this, we directly investigated the molecular signature of mice that naturally recovered after stroke. By directly comparing the molecular responses between naturally recovered and nonrecovered stroke mice, this unperturbed approach may reveal novel mechanisms that have been masked by studies using external restorative therapies. Our study is designed to (1) observe a natural, spontaneous recovery of function in mice after stroke; (2) use unbiased cluster analysis to determine the presence of distinct recovery groups; (3) conduct a novel in-depth lesion analysis to determine if the differential recovery outcome was related to lesion size/locations; (4) use next-generation RNA-sequencing (RNA-seq) technology to investigate the transcriptome of both ipsilesional primary motor cortex (iM1) and contralesional primary motor cortex (cM1) in recovered and nonrecovered stroke mice. Understanding the intrinsic mechanisms driving spontaneous recovery will be invaluable for the development of drugs targeting these mechanisms to promote recovery after stroke.

Methods

Below are the main methods necessary to comprehend the results (details in the online-only Data Supplement). Data supporting the findings of this study are available from the corresponding author on reasonable request.

Animals

All animals used in this study were C57BL/6J wild-type male mice (11–13 weeks of age). To keep the consistency of same gender, female mice were not used in this discovery study. A total of 75 mice were used in this study, of which 33 stroke mice and 7 nonstroke sham mice were included for analysis (Figure I in the online-only Data Supplement for inclusion/exclusion criteria). All experiments were conducted in compliance with animal care laws and institutional guidelines and approved by the Stanford Institutional Animal Care and Use Committee. Mice were randomized and subjected to transient middle cerebral artery occlusion for 30 minutes. All behavior tests were performed by blinded observers on the day before stroke surgery and on poststroke day (PD) 4, 8, and 14.

Semiautomated Lesion Analysis (Magnetic Resonance Imaging, Histology)

A subset of stroke mice was scanned at PD2 using 7-Tesla magnetic resonance imaging (MRI) system. T2-weighted images (T2WI) were acquired and used to quantify the individual infarct volume. For histology, stroke mice were euthanized at PD15 and processed for immunostaining to visualize infarct. Using our pipeline, MRI-based and immunostaining-based images were registered with the Allen brain reference mouse atlas (ARA), and lesion masks were overlaid with the corresponding ARA labels for quantification of infarct volume (MRI) or size (immunostaining).

RNA-Seq Analysis

A subset of stroke mice was selected and their primary motor cortices (ipsilesional and contralesional) were processed for RNA-seq transcriptome analysis using Hiseq 4000 (Illumina, Hayward, CA). Raw sequences were processed for quality control, trimming (Trimmomatic version 0.36), and alignment (STAR/2.5.1b). Downstream analyses were performed using R (version 3.1.1), with edgeR and limma package with voom method. Differentially expressed genes (DEGs) were further analyzed by Ingenuity Pathway Analysis (IPA) software (QIAGEN) to provide the significant canonical pathway, diseases, and functions. Quantitative real-time PCR (qPCR) was used to validate the expression of candidate genes relative to sham group.

Statistical Analysis

For the horizontal rotating beam data (distance and speed data), we performed unsupervised hierarchical clustering analysis (H-clustering) to determine presence of distinct clusters. In addition, gap statistics (clusGap function in R) was used to estimate the number of clusters in all 33 stroke mice included for the analysis. Gap statistics have been previously demonstrated to outperform other methods in estimating the number of clusters in a given data set.[21] For pathway analysis, statistical tests were performed by the Ingenuity Pathway Analysis software using Fisher exact test. Prism 7.03 (GraphPad Software, Inc, La Jolla, CA) was used to perform statistics for the following results. For the quantification of infarct size (% infarct-volume by T2WI or -area by histology) or infarct location (% infarct-volume or -area per region) data, we performed either 2-tailed unpaired Student *t* test or 2-way ANOVA followed by Bonferroni post hoc test. Spearman correlation analysis was used for (1) thalamic lesion and recovery; (2) RNA-seq–based gene expression and recovery; and (3) infarct size and recovery. For qPCR studies, 1-way ANOVA followed by Bonferroni test was used to analyze relative gene expression level to nonstroke sham mice. Significance level was set at $P<0.05$.

Results

Cluster Analysis of the Horizontal Rotating Beam Test Revealed 2 Distinct Recovery Groups

After stroke, we observed the sensory-motor recovery using established behavior tests (see experimental timeline and design in Figure 1A). We chose the horizontal rotating beam test as the primary test because it has been previously demonstrated as a reliable and sensitive test for detecting long-term deficit after stroke.[22,23] Distance data were used for cluster analysis, as it is the most fundamental and unbiased measure of the rotating beam test. We performed unsupervised hierarchical clustering analysis using the distance data from the horizontal beam test. Cluster analysis indicated the emergence of 2 distinct recovery groups at PD14 (Figure 1B): a spontaneously recovered group (n=9) and a nonrecovered group (n=24; Figure 1C and 1D). Nonstroke sham behavior data were included as a comparison. All subsequent analyses were performed based on this group separation, including body weight, vertical stationary beam test, and mNS data (Figure II in the online-only Data Supplement).

Infarct Size and Location Did Not Differ Between Recovery and Nonrecovery Groups

Next, we examined whether the differential recovery outcome between recovered and nonrecovered groups was because of variations in the infarct size and location. Using a semi-automated in-depth lesion mapping analysis, we performed

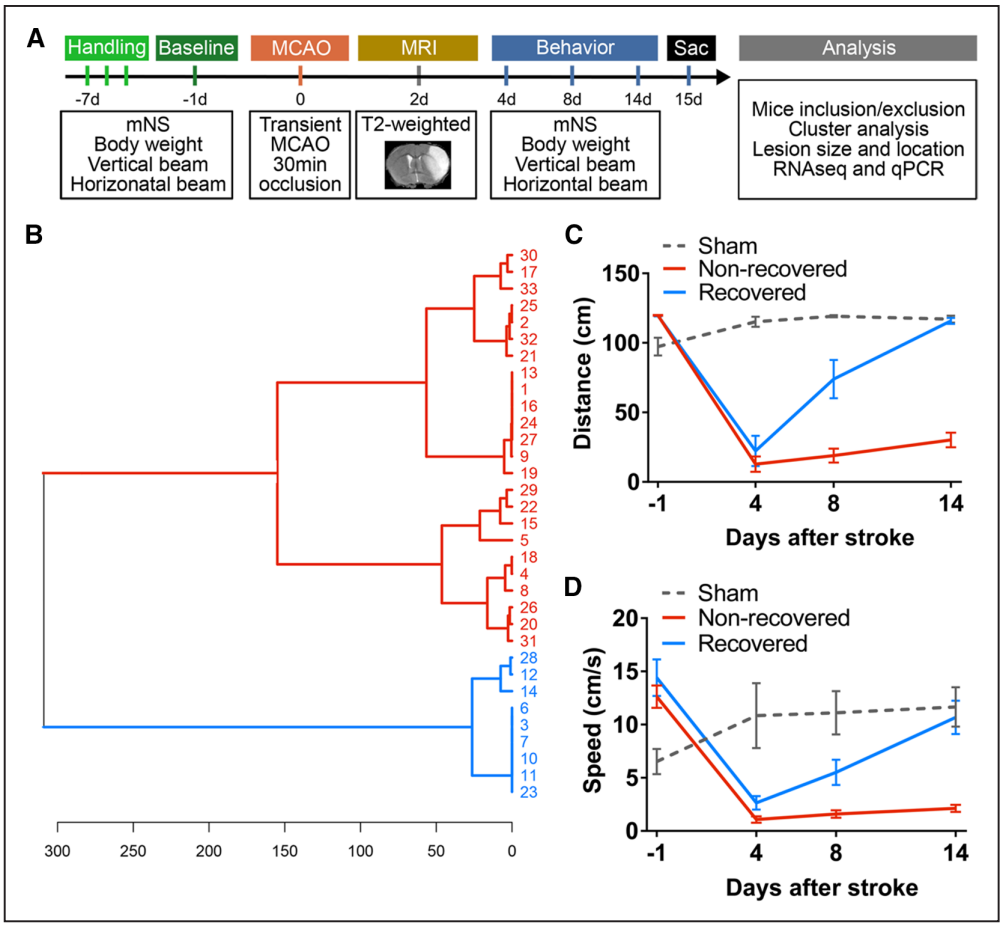

Figure 1. Hierarchical clustering shows 2 distinct recovery groups with differential functional outcome after stroke. **A**, Experimental design and timeline. Mice were trained with several behavior tests 1 week before stroke. These tests included the horizontal rotating beam test, vertical stationary beam test, and modified neurological score (mNS). Baseline performance data were collected at 1 day before stroke (transient middle cerebral artery occlusion [MCAO]) and functional recovery was evaluated at poststroke days (PD) 1, 4, 8, and 14. T2-weighted magnetic resonance imaging (MRI) was acquired at PD2 to visualize the infarct. Mice were euthanized (sac) at PD15 for analyses, including cluster analysis of behavior data, lesion profile, RNA-sequencing (RNA-seq) transcriptome and quantitative real-time PCR (qPCR) validations. **B**, Unsupervised hierarchical cluster dendrogram shows 2 distinct groups of stroke mice (distance metric: Euclidean [horizontal axis], linkage rule: Ward method, vertical axis indicates individual 33 mice IDs included for analysis), computed based on the rotating beam distance performance at PD14. **C**–**D**, Based on this cluster separation, we graphed their rotating beam performance data in distance (**C**) and speed (**D**). Data were expressed as mean±SEM. (n=9 recovered, n=24 nonrecovered, n=7 sham).

a comprehensive evaluation on the infarct size and location of the 2 recovery groups. Cerebral infarcts were visualized either by T2WI at PD2 (Figure 2) in 22 mice or by histology at PD15 by CD68 and MAP2 (microtubule associated protein 2) immunostaining (Figure 3) in the remaining 11 mice. T2WI sequence parameters were listed in Table I in the online-only Data Supplement, and the coregistrations for MRI/histology to ARA were shown in Figure III in the online-only Data Supplement. Our analysis indicated that there was no significant difference in % infarct volume (measured by T2WI on PD2; Figure 2B; P=0.533) or % infarct area (measured by histology at PD15 at the striatal [Str] and thalamohippocampal [Hpx] levels between the groups; Figure 3B; P=0.794 Stx level, P=0.356 Hpx level), although the variation in sample size between the groups could mask any significance in the infarct volume. Overall the incidence of brain regions affected by stroke was similar between recovered and nonrecovered, with a trend toward involvement of a larger portion of the medial thalamus in nonrecovered (Figures 2C and 3C). However, in the voxel-wise analysis, there was no significant difference in lesion location quantified by MRI or histology (Figures 2D and 3D). Nevertheless, we examined whether thalamic lesions can affect behavior outcome. Correlation analysis of thalamic lesions and behavior outcome showed that there was no significant correlation (Figure IV in the online-only Data Supplement). Furthermore, there was no significant correlation between infarct size at PD2 and recovery (Spearman r=–0.112; P=0.621); however, we found a trend of negative correlation between infarct size at PD15 and recovery (Spearman r=–0.545; P=0.086; Figure V in the online-only Data Supplement).

RNA-Seq Transcriptome Analysis in Recovered and Nonrecovered Stroke Mice

We analyzed the transcriptome of iM1 and cM1 in recovered and nonrecovered stroke mice using RNA-seq. The rotating beam behavior results for the 8 stroke mice analyzed with RNA-seq were shown in Figure 4A (recovered, n=3; nonrecovered, n=5). T2WI at PD2 indicated that both groups exhibited comparable cerebral infarcts (Figure 4B, left). For the

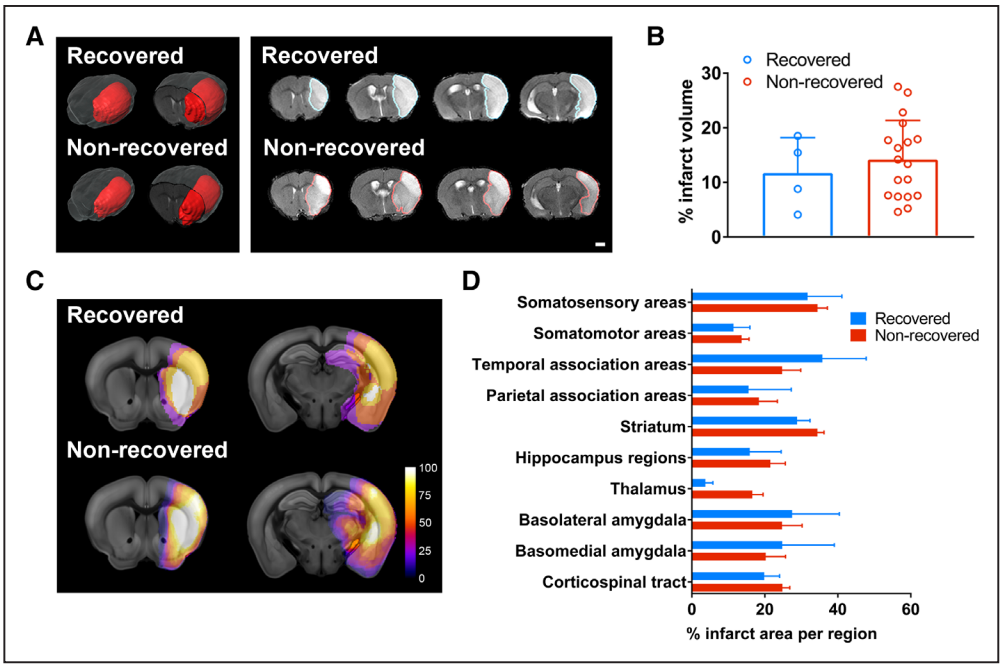

Figure 2. Magnetic resonance imaging analysis of lesion volume and location in recovered and nonrecovered mice at poststroke day 2. **A**, Representative 3-dimensional (3D) visualization of T2-weighted images with segmented stroke lesion masks (red) in the **left**, and 2D coronal images in the **right** for both groups. Scale bar=1 mm. **B**, Bar graph demonstrates mean % infarct volume over whole brain volume. Data were expressed as mean±SEM with individual plots. (n=4 recovered, n=18 nonrecovered). **C**, Voxel-wise incidence maps at the striatal and hippocampal levels were shown. Stroke lesion was expressed as color map (% of mice with stroke lesion) overlaid to the Allen brain reference mouse atlas (ARA). **D**, Semiautomated analysis of % infarct volume per representative ARA region for the quantitative comparison of the lesion location between groups. Data were expressed as mean±SEM. (n=4 recovered, n=18 nonrecovered).

RNA-seq study, mice were euthanized at PD15, and the iM1 and cM1 were dissected (Figure 4B, right) and processed for RNA-seq. Unsupervised cluster analysis by multidimensional scaling plots of the transcriptome profile showed distinct cluster between iM1 and cM1 samples regardless of recovery outcome (Figure 4C, left). Despite the lack of primary ischemic injury in iM1, the unsupervised transcriptome profiling indicated that the transcriptome profile of the primary motor cortex was predominantly affected by stroke.

Supervised hierarchical clustering analysis of the iM1 and cM1 samples (imposed minimum threshold: $P<0.05$) showed distinct cluster separation in cM1 that corresponded to recovered and nonrecovered group (Figure 4C, right). However, cluster analysis of iM1 samples showed 3 groups (Figure 4C, middle), despite similar cerebral infarct. Heat maps and the top upregulated and downregulated genes in iM1 and cM1 were shown in Figure 4D, respectively. Differential transcriptome analysis revealed 263 DEGs in the iM1 (131 upregulated and 132 downregulated; Figure 4D, left) and 417 DEGs in the cM1 (147 upregulated and 270 downregulated; Figure 4D, right) in the recovered group. Top significant upregulated or downregulated genes in the iM1 or cM1 of the recovered group were highlighted in Figure 4D (Table II in the online-only Data Supplement for the full gene name).

RNA-Seq Transcriptome Analysis Highlights Distinct Pathways in the Contralesional Motor Cortex of Recovered Stroke Mice

To further investigate the molecular mechanisms driving spontaneous recovery, we used Ingenuity Pathway Analysis to analyze the DEGs in both iM1 and cM1 (imposed minimum threshold: $P<0.05$, absolute expression log fold change >0.26) and reported relevant canonical pathways, major diseases, molecular and cellular functions (Figure 5). Canonical pathways in the iM1 include the planar cell polarity pathway, axonal guidance signaling, and BMP (bone morphogenetic protein) signaling. Major diseases, molecular and cellular functions in the iM1 include organismal injuries and abnormalities, cell death and survival, cellular growth and proliferation, cell development, cell signaling, and behavior. Other significant canonical pathways in the iM1 include the adipogenesis pathway, TGF-β (transforming growth factor-β) signaling, complement system, p38 MAPK (mitogen-activated protein kinase) signaling, leukocyte extravasation signaling, cAMP-mediated signaling and Wnt/Calcium (Ca+) signaling (Figure 5A).

Canonical pathways in the cM1 included axonal guidance signaling, Wnt/Ca+ pathway and cAMP-mediated signaling (Figure 5B). Major diseases and molecular and cellular functions in the cM1 include organismal injuries and abnormalities, cardiovascular disease, neurological disease, cellular movement, cellular growth and proliferation, and immune cell trafficking. Other significant canonical pathways in the cM1 included prostanoid biosynthesis, eicosanoid signaling, agranulocyte adhesion and diapedesis, ILK (integrin-linked kinase) signaling, GPCR (G protein-coupled receptor) signaling, leukocyte extravasation signaling, and epithelial adherens junction signaling (Figure 5B).

Genes in the cAMP-Mediated Signaling Pathway Are Significantly Correlated With Recovery

To identify genes that may underlie spontaneous recovery, we examined which DEGs were correlated with recovery

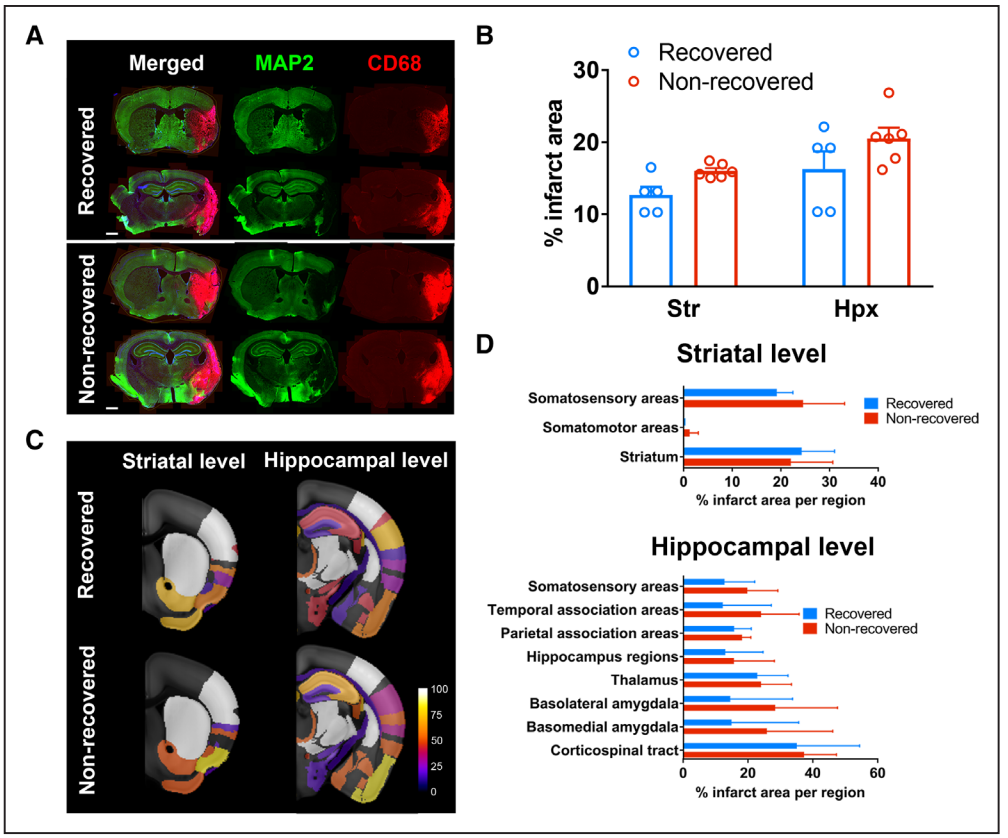

Figure 3. Histological analysis of lesion size and location in recovered and nonrecovered mice at poststroke day (PD) 15. **A**, Representative coronal brain images of MAP2 (microtubule associated protein 2; green) and CD68 (red) immunostaining at the striatal (Str) and thalamo-hippocampal (Hpx) levels from recovered and nonrecovered mice at PD15. Note that the CD68-positive area was predominantly overlaid on the MAP2-negative neuronal loss area in the merged images. Scale bar=1 mm. **B**, Bar graph demonstrated the average % infarct area over the whole brain section area (mean±SEM; n=5 recovered, n=6 nonrecovered). **C**, Incidence maps at the striatal and hippocampal levels were shown. Stroke lesion was expressed as color map (% of mice with stroke lesion) overlaid to the Allen brain reference mouse atlas (ARA). **D**, Semiautomated quantification of % infarct area per selected region at Str (upper) and Hpx (lower) level, respectively. Data were expressed as mean±SEM (n=5 recovered, n=6 nonrecovered).

by performing correlation analysis between gene expression level (counts per million reported from RNA-seq analysis) of each DEG and behavior recovery outcome (distance data at PD14 from the rotating beam test). Correlation analysis indicated that there were 38 DEGs in the iM1 and 74 DEGs in the cM1 correlated with recovery (Tables III and IV in the online-only Data Supplement). We focused our subsequent analysis in the cM1 because (1) more DEGs in cM1 were correlated with recovery and (2) more distinct separation was found in the supervised hierarchical clustering analysis of the cM1 samples instead of the iM1 samples. Ingenuity Pathway Analysis of the 74 DEGs in cM1 revealed cAMP-mediated signaling as the first top significant canonical pathway (Figure 5C, right), with all 4 DEGs (Adora2a [adenosine receptor A2A], Drd2 [dopamine receptor D2], Pde10a [phosphodiesterase 10A], and Ptger4 [prostaglandin E receptor 4]) significantly downregulated in recovered mice (Table IV in the online-only Data Supplement). These 4 DEGs were all significantly and negatively correlated with functional recovery (Figure 5D). Interestingly, cAMP-mediated signaling was also included in the top 10 relevant canonical pathways in the iM1 (Figure 5A). In iM1, there was no difference in Adora2a and Drd2 between recovered and nonrecovered mice (P>0.10), whereas Pde10a expression was significantly decreased (log FC=−0.217, P=0.015) and Ptger4 was significantly increased (log FC=0.628, P=0.033) in the recovered mice. Most of these 4 genes (except for Pde10a) in the iM1 were not significantly correlated with functional recovery.

qPCR Verification of Candidate Genes in the cAMP Signaling Pathway

Next, we used qPCR to validate the 4 DEGs in the cAMP pathway in cM1. qPCR successfully validated 3 out of 4 genes in this pathway, namely Adora2a, Drd2, and Pde10a (Figure 6). Both Adora2a and Drd2 were significantly upregulated in nonrecovered stroke mice when compared with nonstroke sham mice. Interestingly, Adora2a, Drd2, and Pde10a were significantly reduced in recovered mice, to a level similar to sham. As Adora2a, Drd2, and Pde10a are known to be highly expressed in the striatum,[24–26] we also examined their expression in the contralesional somatosensory cortex and striatum. Interestingly, all 3 genes were selectively decreased in the cM1 of recovered mice, but not in contralesional somatosensory cortex nor contralesional somatosensory striatum (Figure 6).

Discussion

To our knowledge, this is the first study to investigate the molecular signature in the motor cortex of stroke mice that

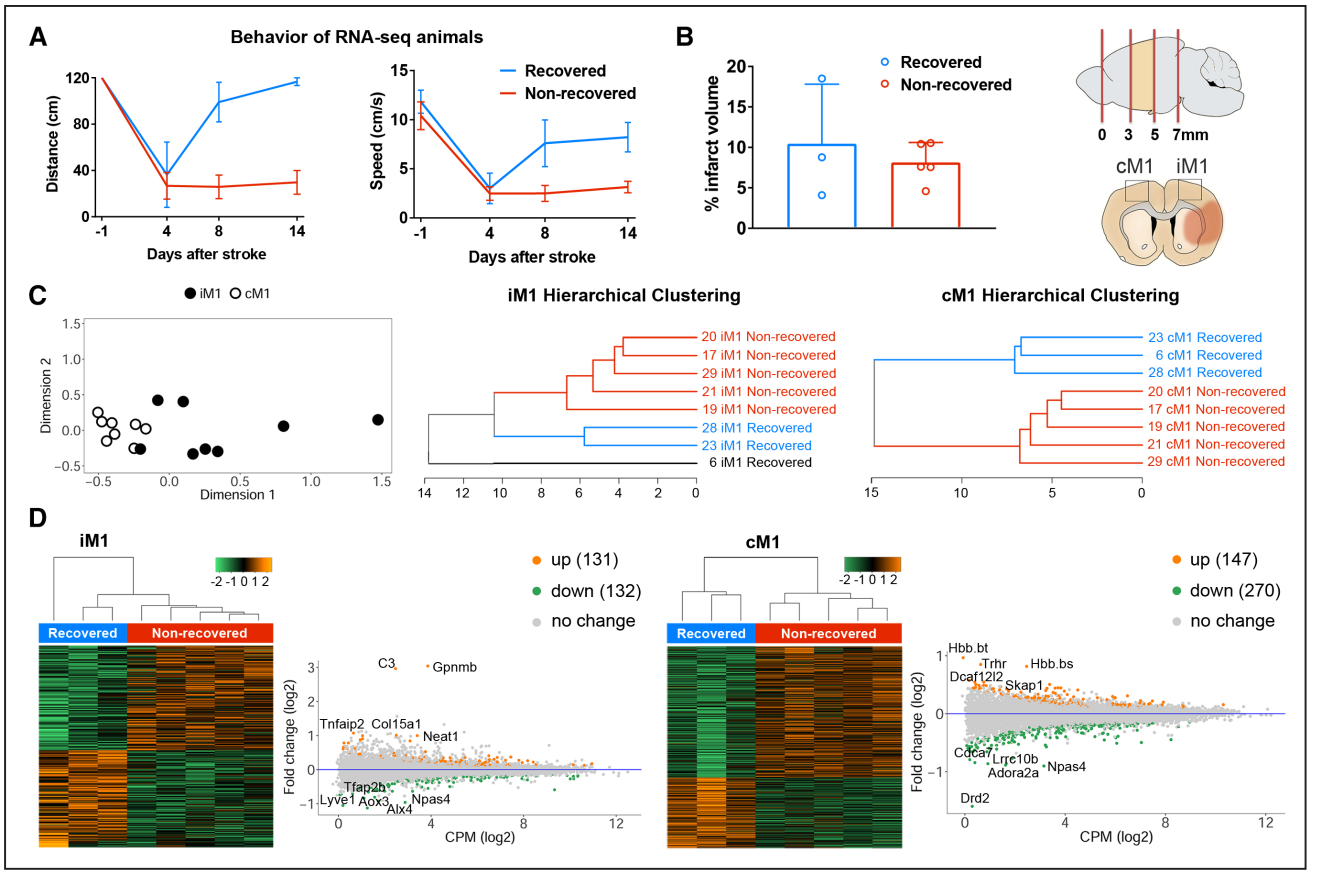

Figure 4. RNA-sequencing (RNA-seq) transcriptome analysis of ipsilesional primary motor cortex (iM1) and contralesional primary motor cortex (cM1) in recovered and nonrecovered mice. **A**, Rotating beam results (distance and speed) for the mice used in RNA-seq analysis. **B**, Bar graph demonstrates mean % infarct volume over whole brain volume for these mice. Data were expressed as mean±SEM (n=3 recovered, n=5 nonrecovered mice). Schematic diagram for the dissections of the brain cortical regions. Coronal brain image depicted cerebral infarct (orange colored). iM1 and cM1 were dissected and processed for RNA-seq analysis. **C**, Unsupervised multidimensional scaling plot for the iM1 and cM1 samples from both recovered and nonrecovered mice (n=3 and 5 mice, respectively) was shown on **left**. Supervised hierarchical clustering dendrograms of the differentially expressed genes (DEG, $P<0.05$) in the iM1 and cM1 were shown in the **middle** and **right**. **D**, Heatmaps and MA plots (M=log ratio and A=mean average) of transcriptome gene expressions in iM1 and cM1 samples from both groups, respectively. Orange and green dots in the MA plots indicated top differentially upregulated and downregulated genes ($P<0.05$) in recovered mice, respectively.

naturally recovered without external intervention. By directly comparing the molecular responses between naturally recovered and nonrecovered stroke mice, our approach may reveal novel molecular signature that have been masked by studies using external restorative treatments. Our data showed that stroke mice with comparable infarcts can exhibit differential functional recovery outcomes. RNA-seq transcriptome analysis revealed distinct biological pathways in both the iM1 and cM1 of recovered stroke mice. Our RNA-seq analysis showed that multiple pathways in the iM1 and cM1 are likely to be involved in mediating spontaneous recovery after stroke. Canonical pathways in the iM1 include the axonal guidance signaling, BMP signaling, TGF-β signaling, complement system, MAPK signaling, leukocyte extravasation signaling, cAMP-mediated signaling, and Wnt/Calcium signaling (Figure 5). Most of these pathways in the iM1 are consistent with our knowledge of brain repair pathways after stroke and have been shown to have neuroprotective and neurodegenerative roles.[27] Importantly, our RNA-seq data revealed a panel of spontaneous recovery-related genes (Figures 4 and 5) and reported the involvement of novel biological pathways in cM1. In particular, the cAMP-mediated signaling pathway in the cM1 was highlighted (Figure 5C, right), with the recovered stroke mice exhibiting a significantly lower expression of 2 GPCRs (Adora2a and Drd2) and Pde10a, to a level similar to sham. Interestingly, the expression of these genes in the cM1 is negatively correlated with behavioral recovery. Our study suggests that Adora2a, Drd2, and Pde10a-mediated signaling may be important for spontaneous recovery after stroke.

To further hone in on the key molecules that mediate spontaneous recovery, we focused on DEGs that were significantly correlated with behavior performance. We have identified a panel of recovery-related genes in both iM1 and cM1 (Tables III and IV in the online-only Data Supplement). Notably, the cAMP-mediated pathway was the first top pathway highlighted in the cM1, with 4 DEGs (Adora2a, Drd2, Pde10a, and Ptger4) significantly downregulated in the recovered mice, and their expressions were negatively correlated with recovery (Figure 5C, right; Figure 5D). Of these 4 genes, we have successfully validated Adora2a, Drd2, Pde10a using qPCR (Figure 6). Interestingly, these genes were selectively decreased in the cM1 of recovered stroke mice, but not in contralesional somatosensory cortex

A

IPA iM1 Pathway Analysis

Canonical Pathways	Diseases, Molecular & Cellular Functions	
PCP Pathway	Organismal Injuries and Abnormalities	Cell Development
Axonal Guidance Signaling	Cell Death and Survival	Cell Signaling
BMP signaling	Cellular Growth and Proliferation	Behavior

B

IPA cM1 Pathway Analysis

Canonical Pathways	Diseases, Molecular & Cellular Functions	
Axonal Guidance Signaling	Organismal Injuries and Abnormalities	Cellular Movement
Wnt/Ca+ pathway	Cardiovascular Disease	Cellular Growth and Proliferation
cAMP-mediated signaling	Neurological Disease	Immune Cell Trafficking

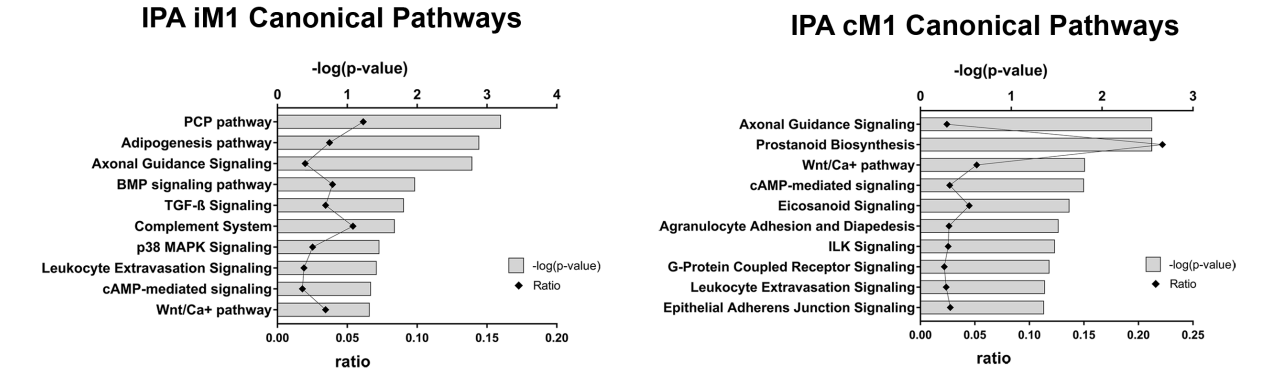

C

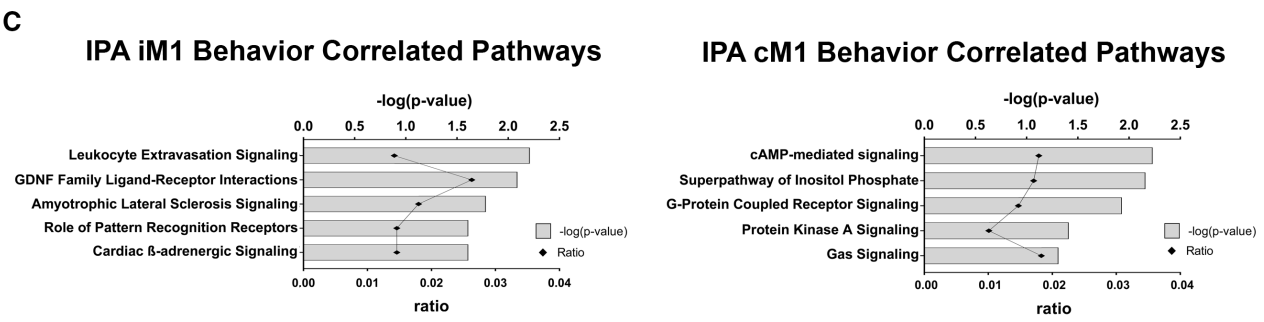

D

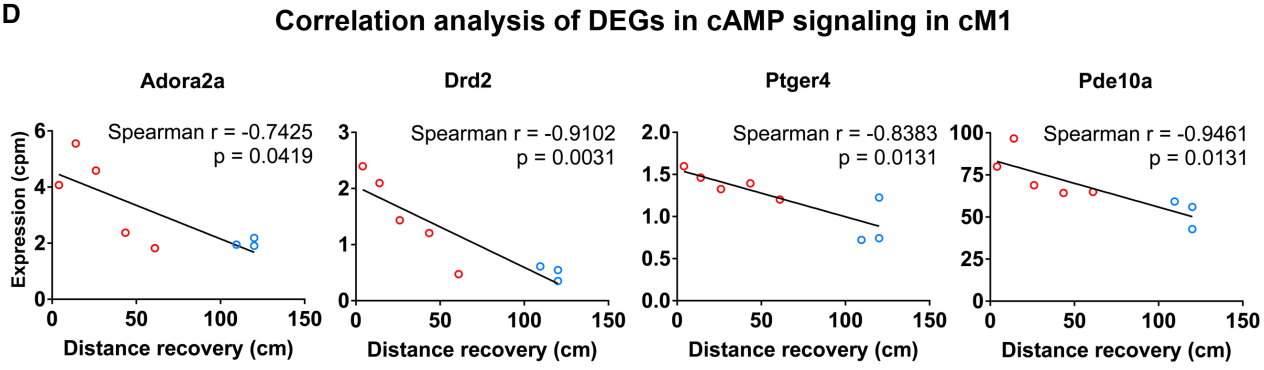

Figure 5. Ingenuity pathway analysis (IPA) of RNA-sequencing (RNA-seq) transcriptome highlights the involvement of cAMP-mediated signaling in the contralesional primary motor cortex (cM1). **A**–**B**, IPA of differentially expressed genes (DEGs) in the (**A**) ipsilesional primary motor cortex (iM1) or (**B**) cM1 (upper tables) in recovered stroke mice indicated significant top canonical pathways and diseases, molecular/cellular functions. Bar graphs indicated significant top canonical pathways in (**A**) iM1 and (**B**) cM1 (lower graphs), plotted by *P* values (Fisher exact test) and ratio (number of genes in pathway). **C**, Bar graphs demonstrate significant top 5 relevant canonical pathways correlated with recovery in the iM1 (**left**) and cM1 (**right**). **D**, Scatter plots demonstrated significant negative correlations (Spearman) between gene expression levels (RNA-seq counts per million based) of 4 DEGs in cAMP-mediated signaling in the cM1 (Adora2a [adenosine receptor A2A], Drd2 [dopamine receptor D2], Ptger4 [prostaglandin E receptor 4], and Pde10a [phosphodiesterase 10A]) and the behavior recovery outcome (rotating beam distance at poststroke day 14). Each line depicted linear regression for each scatter plot (n=3 recovered, n=5 nonrecovered mice). BMP indicates bone morphogenetic protein; and PCP, planar cell polarity.

nor contralesional somatosensory striatum. The functions of these genes are briefly discussed below.

Both Adora2a and Drd2 have been studied in acute stroke,[28–31] however, their role in the brain repair and recovery is unclear, because there are no reports of its role in chronic stage of stroke. Adora2a is a Gs-protein coupled that activates the cAMP-mediated signaling pathway.[32] It has been shown that blocking Adora2a signaling can protect against acute

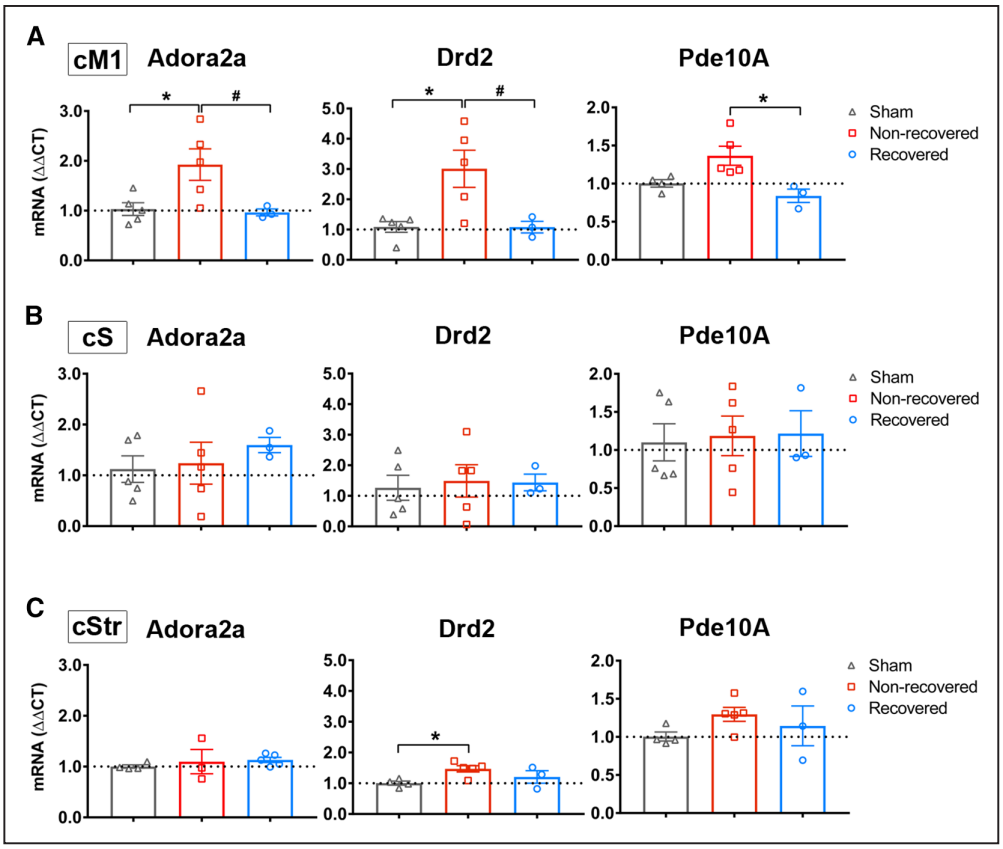

Figure 6. Adora2a (adenosine receptor A2A), Drd2 (dopamine receptor D2), and Pde10a (phosphodiesterase 10A) were selectively decreased in contralesional primary motor cortex (cM1) of recovered mice. **A**–**B**, Quantitative real-time PCR (qPCR) verification of Adora2a (**A**), Drd2 (**B**), and Pde10a (**C**) mRNA expression in recovered and nonrecovered stroke mice and nonstroke sham mice in each region: cM1 (upper), contralesional somatosensory cortex (cS; **middle**), and contralesional somatosensory striatum (cStr; lower). Graphs indicated gene expression levels relative to sham group. GAPDH was used as reference gene. Data were expressed as mean ΔΔCT±SEM. The dotted horizontal line indicates ΔΔCT=1.0. **P*<0.05 1-way ANOVA, followed by Bonferroni test indicates a significant difference from sham (n=5), and #*P*<0.05 indicates a significant difference between recovered (n=3) and nonrecovered group (n=5).

ischemic excitotoxicity, whereas activating Adora2a signaling within a few hours poststroke can reduce inflammatory cell infiltration after stroke.[28] However, Drd2 is a Gi protein-coupled receptor that inhibits cAMP-mediated signaling.[33] The dopamine system plays a key role in motor learning and neuroplasticity.[34,35] A recent study showed that activation of Drd2 on astrocytes in acute stroke can reduce neuroinflammation.[31] However, the role of Drd2 in brain repair is also unclear. On the other hand, the role of Pde10a in stroke has not been reported. Recent studies showed that inhibition of Pde10a may be a promising therapeutic strategy for psychiatric and neurodegenerative diseases.[36] Our RNA-seq analysis highlights these genes as potential targets for enhancing stroke recovery; however, the functional consequences of these genes will depend on which cell type showed reduction of these genes in recovered stroke mice, as well as the effects of selective modulations of their signaling in cM1 on recovery outcome. Future studies are required to elucidate the role of these genes in spontaneous recovery and to address whether they act through neuroinflammatory and neuroplasticity mechanisms.

In conclusion, we reported the first RNA-seq transcriptome in the motor cortex of stroke mice that naturally recovered and unraveled the intrinsic molecular signature of spontaneous recovery after stroke in mice. We revealed a panel of recovery-related genes and highlighted canonical pathways in the cM1 of recovered stroke mice, specifically the cAMP-mediated signaling pathway involving Adora2a, Drd2, and Pde10a. Our data indicate that Adora2a, Drd2, and Pde10a signaling in the cM1 may play important roles in stroke recovery. Developing drugs that target these candidates during different phases of recovery may provide beneficial recovery outcome in stroke patients.

Acknowledgments

We thank Drs Brad Efron, John S. Tamaresis, and Balasubramanian Narasimhan (Department of Statistics at Stanford University) for discussion on Gap statistics cluster analysis. We also thank Anika Kim and Lorenzo Gonzalez for assistance in behavior studies and immunostaining. We thank Dr Tonya Bliss for helpful discussions on the article. We thank Cindy H. Samos for scientific editing of the article.

Sources of Funding

This study was supported in part by National Institutes of Health (NIH) National Institute of Neurological Disorders and Stroke grants R21NS082894 and R01NS093057, Russell and Elizabeth Siegelman, and Bernard and Ronni Lacroute (to Dr Steinberg); partly supported by R01NS095985 and R01 MH111444 (to Dr McNab), NIH S10 Shared Instrumentation Grant (S10RR026917-01 to Dr Michael Moseley); and postdoctoral fellowships from the Japan Society for the Promotion of Science and the SENSHIN Medical

Research Foundation (to Dr Ito) and the Max Kade Foundation (to Dr Aswendt). Dr Steinberg is a consultant for Qool Therapeutics, Peter Lazic US, Inc, and NeuroSave.

Disclosures

None.

References

1. Feigin VL, Forouzanfar MH, Krishnamurthi R, Mensah GA, Connor M, Bennett DA, et al; Global Burden of Diseases, Injuries, and Risk Factors Study 2010 (GBD 2010) and the GBD Stroke Experts Group. Global and regional burden of stroke during 1990-2010: findings from the Global Burden of Disease Study 2010. *Lancet*. 2014;383: 245–254.
2. Cramer SC, Wolf SL, Adams HP Jr, Chen D, Dromerick AW, Dunning K, et al. Stroke recovery and rehabilitation research: issues, opportunities, and the National Institutes of Health StrokeNet. *Stroke*. 2017;48:813–819. doi: 10.1161/STROKEAHA.116.015501
3. Ward NS. Mechanisms underlying recovery of motor function after stroke. *Postgrad Med J*. 2005;81:510–514. doi: 10.1136/pgmj.2004.030809
4. Ward NS. Restoring brain function after stroke - bridging the gap between animals and humans. *Nat Rev Neurol*. 2017;13:244–255. doi: 10.1038/nrneurol.2017.34
5. Rothrock JF, Clark WM, Lyden PD. Spontaneous early improvement following ischemic stroke. *Stroke*. 1995;26:1358–1360.
6. Whishaw IQ. Loss of the innate cortical engram for action patterns used in skilled reaching and the development of behavioral compensation following motor cortex lesions in the rat. *Neuropharmacology*. 2000;39:788–805.
7. Cramer SC. Repairing the human brain after stroke: I. Mechanisms of spontaneous recovery. *Ann Neurol*. 2008;63:272–287. doi: 10.1002/ana.21393.
8. Cassidy JM, Cramer SC. Spontaneous and therapeutic-induced mechanisms of functional recovery after stroke. *Transl Stroke Res*. 2017;8:33–46. doi: 10.1007/s12975-016-0467-5
9. Liu XS, Zhang ZG, Zhang RL, Gregg S, Morris DC, Wang Y, et al. Stroke induces gene profile changes associated with neurogenesis and angiogenesis in adult subventricular zone progenitor cells. *J Cereb Blood Flow Metab*. 2007;27:564–574. doi: 10.1038/sj.jcbfm.9600371
10. Brown CE, Li P, Boyd JD, Delaney KR, Murphy TH. Extensive turnover of dendritic spines and vascular remodeling in cortical tissues recovering from stroke. *J Neurosci*. 2007;27:4101–4109. doi: 10.1523/JNEUROSCI.4295-06.2007.
11. Carmichael ST, Archibeque I, Luke L, Nolan T, Momiy J, Li S. Growth-associated gene expression after stroke: evidence for a growth-promoting region in peri-infarct cortex. *Exp Neurol*. 2005;193:291–311. doi: 10.1016/j.expneurol.2005.01.004
12. Carmichael ST, Kathirvelu B, Schweppe CA, Nie EH. Molecular, cellular and functional events in axonal sprouting after stroke. *Exp Neurol*. 2017;287(pt 3):384–394. doi: 10.1016/j.expneurol.2016.02.007
13. Caleo M. Rehabilitation and plasticity following stroke: Insights from rodent models. *Neuroscience*. 2015;311:180–194. doi: 10.1016/j.neuroscience.2015.10.029
14. Madinier A, Bertrand N, Rodier M, Quirié A, Mossiat C, Prigent-Tessier A, et al. Ipsilateral versus contralateral spontaneous post-stroke neuroplastic changes: involvement of BDNF? *Neuroscience*. 2013;231:169–181. doi: 10.1016/j.neuroscience.2012.11.054
15. George PM, Steinberg GK. Novel stroke therapeutics: unraveling stroke pathophysiology and its impact on clinical treatments. *Neuron*. 2015;87:297–309. doi: 10.1016/j.neuron.2015.05.041
16. Webster BR, Celnik PA, Cohen LG. Noninvasive brain stimulation in stroke rehabilitation. *NeuroRx*. 2006;3:474–481. doi: 10.1016/j.nurx.2006.07.008
17. Barone FC. Post-stroke pharmacological intervention: promoting brain recovery from injury in the future. *Neuropharmacology*. 2010;59:650–653. doi: 10.1016/j.neuropharm.2010.08.016
18. Silasi G, Murphy TH. Stroke and the connectome: how connectivity guides therapeutic intervention. *Neuron*. 2014;83:1354–1368. doi: 10.1016/j.neuron.2014.08.052
19. Grefkes C, Fink GR. Reorganization of cerebral networks after stroke: new insights from neuroimaging with connectivity approaches. *Brain*. 2011;134(Pt 5):1264–1276. doi: 10.1093/brain/awr033
20. Lim DH, LeDue JM, Mohajerani MH, Murphy TH. Optogenetic mapping after stroke reveals network-wide scaling of functional connections and heterogeneous recovery of the peri-infarct. *J Neurosci*. 2014;34:16455–16466. doi: 10.1523/JNEUROSCI.3384-14.2014
21. Tibshirani R, Walther G, Hastie T. Estimating the number of clusters in a data set via the gap statistic. *J R Stat Soc Series B Stat Methodol*. 2001;63:411–423.
22. Cheng MY, Wang EH, Woodson WJ, Wang S, Sun G, Lee AG, et al. Optogenetic neuronal stimulation promotes functional recovery after stroke. *Proc Natl Acad Sci USA*. 2014;111:12913–12918. doi: 10.1073/pnas.1404109111
23. Shah AM, Ishizaka S, Cheng MY, Wang EH, Bautista AR, Levy S, et al. Optogenetic neuronal stimulation of the lateral cerebellar nucleus promotes persistent functional recovery after stroke. *Sci Rep*. 2017;7:46612. doi: 10.1038/srep46612
24. Svenningsson P, Le Moine C, Fisone G, Fredholm BB. Distribution, biochemistry and function of striatal adenosine A2A receptors. *Prog Neurobiol*. 1999;59:355–396.
25. Pignatelli M, Bonci A. Role of dopamine neurons in reward and aversion: a synaptic plasticity perspective. *Neuron*. 2015;86:1145–1157. doi: 10.1016/j.neuron.2015.04.015
26. Xie Z, Adamowicz WO, Eldred WD, Jakowski AB, Kleiman RJ, Morton DG, et al. Cellular and subcellular localization of PDE10A, a striatum-enriched phosphodiesterase. *Neuroscience*. 2006;139:597–607. doi: 10.1016/j.neuroscience.2005.12.042
27. Harvey BK, Hoffer BJ, Wang Y. Stroke and TGF-beta proteins: glial cell line-derived neurotrophic factor and bone morphogenetic protein. *Pharmacol Ther*. 2005;105:113–125. doi: 10.1016/j.pharmthera.2004.09.003
28. Pedata F, Pugliese AM, Coppi E, Dettori I, Maraula G, Cellai L, et al. Adenosine A2A receptors modulate acute injury and neuroinflammation in brain ischemia. *Mediators Inflamm*. 2014;2014:805198. doi: 10.1155/2014/805198
29. Melani A, Pugliese AM, Pedata F. Adenosine receptors in cerebral ischemia. *Int Rev Neurobiol*. 2014;119:309–348. doi: 10.1016/B978-0-12-801022-8.00013-1
30. Chen JF, Huang Z, Ma J, Zhu J, Moratalla R, Standaert D, et al. A(2A) adenosine receptor deficiency attenuates brain injury induced by transient focal ischemia in mice. *J Neurosci*. 1999;19:9192–9200.
31. Qiu J, Yan Z, Tao K, Li Y, Li Y, Li J, et al. Sinomenine activates astrocytic dopamine D2 receptors and alleviates neuroinflammatory injury via the CRYAB/STAT3 pathway after ischemic stroke in mice. *J Neuroinflammation*. 2016;13:263. doi: 10.1186/s12974-016-0739-8
32. Dai SS, Zhou YG. Adenosine 2A receptor: a crucial neuromodulator with bidirectional effect in neuroinflammation and brain injury. *Rev Neurosci*. 2011;22:231–239. doi: 10.1515/RNS.2011.020
33. Montmayeur JP, Guiramand J, Borrelli E. Preferential coupling between dopamine D2 receptors and G-proteins. *Mol Endocrinol*. 1993;7:161–170. doi: 10.1210/mend.7.2.7682286
34. Hosp JA, Luft AR. Dopaminergic meso-cortical projections to m1: role in motor learning and motor cortex plasticity. *Front Neurol*. 2013;4:145. doi: 10.3389/fneur.2013.00145
35. Cramer SC. Drugs to enhance motor recovery after stroke. *Stroke*. 2015;46:2998–3005. doi: 10.1161/STROKEAHA.115.007433
36. Zagorska A, Partyka A, Bucki A, Gawalska A, Czopek A, Pawlowski M. Phosphodiesterase 10 inhibitors – novel perspectives for psychiatric and neurodegenerative drug discovery. *Curr Med Chem*. 2018;25.